This full text paper was peer reviewed at the direction of IEEE Communications Society subject matter experts for publication in the WCNC 2007 proceedings.

Adaptive Modulation and Coding for IEEE 802.11n

Fei Peng*, Jinyun Zhang† and William E. Ryan*
*University of Arizona, {*feip,ryan*}*@ece.arizona.edu*
†Mitsubishi Electric Research Laboratories, *jzhang@merl.com*

***Abstract*— We propose a link adaptation technique for IEEE 802.11n MIMO-OFDM systems with convolutional coding. The technique dynamically selects the best modulation and coding scheme (MCS) based on channel conditions and on the medium access control (MAC) layer performance (coded BER or PER) requested by applications. We show that the coded performance at decoder output can be modeled as a function of decoder-input uncoded BER and the code rate. For MIMO-OFDM systems with different modulation types for different spatial streams at each subcarrier, we propose a simple and accurate method for computing the BER for each spatial stream mixed from different subcarriers. We also discuss approaches for searching and selecting the MCS.**

I. Introduction

The emerging IEEE 802.11n standard employs multi-input multi-output orthogonal frequency division multiplexing (MIMO-OFDM) transmission techniques to enable high-throughput communication for up to 600 Mbps in a 40 MHz channel bandwidth [1]. Since the wireless fading channel varies with time, link adaptation must be employed to sustain reliable communication and maximize throughput. The standard defines medium access control (MAC) protocols and a large set of modulation and coding schemes (MCS) to facilitate this goal [1]. In this paper, we present a MAC performance-based link adaptation technique for IEEE 802.11n.

The technique dynamically selects the best MCS based on channel conditions and on the MAC layer performance requested by applications. The performance request here refers to the MAC packet-error rate (PER) or coded bit-error rate (BER). With the CRC-32 [1] code, the physical (PHY) layer PER may be treated approximately identical to MAC PER for practical applications.

IEEE 802.11n implements bit-interleaved coded modulation (BICM) [2]. Adaptive BICM for scalar channels has been well studied [3], where the coded BER can be computed via the trellis codes' transfer function for symbol/block-wise adaptation [4]. For matrix channels, such as the MIMO-OFDM channel in 802.11n, since the channel state information is no longer a scalar, the scalar-channel results can not be directly applied except using the post-processing SNR. In [5], adaptive BICM is studied for MIMO-OFDM channels with beamforming and sub-channel grouping, assuming each spatial channel employs independent BICM streams (i.e. horizontal encoding [6]). Vertical encoding is examined in [7] for turbo-receivers for MIMO channels using EXIT charts [8]. An expurgated bound technique is introduced in [9]. There are also a large number of publications on adaptive modulation and bit-loading (e.g. [10]) where uncoded BER is used as a performance measure. In addition to these analytical approaches, simulation-aided techniques can be found in [11] for OFDM and [12] for MIMO-OFDM, where the adaptation SNR thresholds are determined via simulations.

Despite extensive research effort on adaptive modulation and coding, the techniques in [3]-[7] are dependent on channel fading statistics and are still too complex for practical implementations, especially for systems with a large set of MCS such as 802.11n. For coded systems, the uncoded BER [10] alone is not a useful performance measure, since the coded performance also depends on the code rate. On the other hand, the effectiveness and efficiencies of simulation-based approaches depend heavily on the assumed channel model, and could be problematic in practice, particularly for MIMO-channels.

In this paper, we propose a practical link adaptation technique designed specifically for the 820.11n vertical-encoded BICM-MIMO-OFDM system with and without beamforming. We adopt a minimum mean-square error (MMSE) receiver [13] for the (space-time coded) MIMO channel. Using Gaussian approximation for the MMSE output [14], we derive alternative simple close-form expressions of BER and PER for BICM with M-QAM over the AWGN channel, which can be applied to our situation. We show that the decoder-output BER/PER can be approximated as a function of the decoder-input BER (over all MIMO spatial streams and OFDM subcarriers) and the code rate, which can be optimized for real-time applications. We also propose a simple SNR metric that bypasses the intensive computation of combining uncoded BER from OFDM subcarriers. We demonstrate that the proposed technique [15] can satisfy the PER requirement and also upper limit the average BER for failed packets in simulations.

We briefly review the system model in Section II. The alternative performance bounds of BICM-QAM is presented in Section III. We discuss computation of decoder input-BER in Section IV for MIMO channels with different modulation types on each spatial stream. In Section V, we discuss algorithms for searching and selecting the MCS. In Section VI, we present simulation results. Section VII concludes the paper.

II. System Model

Each MIMO channel carried by an OFDM subcarrier can be expressed as (omitting subcarrier index)

$$\underline{R} = \mathbf{H}\underline{X} + \underline{W} \tag{1}$$

where $\underline{X}$ is a vector of transmitted modulation symbols of unit power [1], $\underline{R}$ is the OFDM demodulator output, and $\underline{W}$ is the channel noise vector whose variance is denoted by N_0. $\mathbf{H}$

1525-3511/07/$25.00 ©2007 IEEE

Authorized licensed use limited to: CLEMSON UNIVERSITY. Downloaded on July 15,2024 at 19:51:40 UTC from IEEE Xplore. Restrictions apply.

Charter Communications, Inc.
Exhibit 1014
Page #1

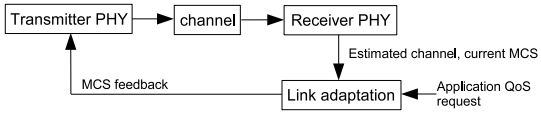

Fig. 1. A brief diagram of the proposed system. Details on 802.11n can be found in [1].

is the equivalent channel matrix, and depends on the channel impulse response, the transmitter cyclic-delay diversity values, and the transmitter spatial mapping (or beamforming) matrices [1]. Its detailed expression is not of concern to this paper, and beamforming is transparent to the techniques proposed here. The propagation channel used in this study is the IEEE indoor frequency-selective slow fading channel model [16].

The number of active spatial streams (modulated independent data streams) of the MIMO channel is denoted by N_{ss}. When space-time block coding (STBC) is employed, two OFDM symbols are processed together for space-time decoding, and (1) should be structured according to the space-time coding scheme [1].

We assume perfect and per-tone channel estimation (per-carrier independent, unsmoothed channel estimate [1]) and MMSE detection of $\underline{X}$ throughout this paper, although the results can be easily extended to other channel estimation and MIMO detection approaches, such as least-squares (LS) channel estimation and VBLAST [18] detection. The MMSE detector outputs log-likelihood ratios (LLRs) (with max-log simplification [17]) that can be used by both Viterbi decoding and belief-propagation decoding.

The overall structure of the proposed system is illustrated in Fig. 1, where the transmitter and receiver PHY implements the vertical-encoded MIMO-OFDM transmission technique as specified in [1]. The proposed link adaptation is implemented on the receiver side. The selected MCS is fed back to the transmitter via mechanisms defined in the MAC protocols [1]. The receiver PHY supplies the estimated channel and MCS of the current packet to the link adaptation unit, which selects the best MCS based on the performance request (denoted by "QoS" in Fig. 1) from the application in terms of coded PER or coded BER. We point out that it is easy to verify via simulations that over the AWGN channel, for different modulation schemes and code rates, coded PER may be approximated as a function of the coded BER. Thus the performance request in coded BER can be converted to decoded PER and vice versa.

III. Bounds on Punctured Convolutional-Coded M-QAM

As we discussed earlier, due to a Gaussian approximation of MMSE output [14], we only need to focus on the AWGN channel when analyzing the BICM performance. Rather than following the complicated bounds in [2], we give simple alternative derivations in this section.

Since it is well known that over the AWGN channel, interleaving does not alter the inherent channel statistics and hence performance, we can simply use the bounds for convolutional-coded M-QAM. Although bounds on punctured convolutional codes (CC) have been well studied in the literature [20], to our knowledge, all existing publications assume BPSK modulation. We derive here tight bounds for punctured convolutional-coded Gray-mapped QAM modulations defined in [1]. We note here that it is also possible to approximate the receiver QAM bit-LLR as a BPSK channel, but with a rather complicated statistical behavior that precludes simple closed-form expressions.

The union upper bound on the BER P_b for a (punctured) rate $R = k_0/n_0$ (k_0, n_0 relative prime) convolutional code is given by $P_b \leq \frac{1}{k_0}\sum_{d=d_{free}}^{\infty} C_d P_d$, where C_d is the number of bit errors for the Hamming weight-d paths, and P_d is the probability that a weight-d sequence is selected over the all-zero sequence. For the industry standard (1/2,7) code used in 802.11n, C_d for different puncturing patterns is well known [20].

Let d_{min} be the minimum Euclidean distance for the signal constellation under discussion. For BPSK, it is well known that $P_d = Q\left(\sqrt{\frac{2dE_s}{N_0}}\right)$. For QPSK, if k of the d bit errors occur in k different QPSK symbols, then it is easy to show that

$$P_d = \sum_{k=0}^{d} \frac{\binom{d}{k}}{2^d} Q\left(\sqrt{\frac{kd_{min}^2 + 2d_{min}^2(d-k)/2}{2N_0}}\right) = Q\left(\sqrt{\frac{dE_s}{N_0}}\right).$$

For 16-QAM and 64-QAM, P_d depends on the bit-mapping and the signal constellation layout. Let k_n ($1 \leq n \leq 4$) be the number of symbols corresponding to n bit-errors per symbol in the symbol sequence mapped from the weight-d binary sequence. To compute the bound on BER at the decoder output, we need to first consider the probability that a weight-d sequence is selected over a weight-0 sequence. Let $\tilde{d}_1^2$ be the equivalent Euclidean distance corresponding to events with one bit error per constellation symbol. For the 16-QAM constellation defined in [1], there are only two possibilities such that one symbol error leads to one bit error. Let P_1 (P_3) be the probability that such a symbol error has distance d_{min} ($3d_{min}$), then $\tilde{d}_1^2 = \frac{1+9P_3/P_1}{1+P_3/P_1} d_{min}^2 \approx d_{min}^2$, where the approximation is accurate for medium-to-high SNR values. Similarly, $\tilde{d}_2^2 \approx 2d_{min}^2$, $\tilde{d}_3^2 \approx 5d_{min}^2$ and $\tilde{d}_4^2 = 8d_{min}^2$. After simplification with $d = \sum_{i=1}^{4} k_i i$ for 16-QAM, P_d can be expressed by

$$P_d \approx \frac{1}{I_d} \sum_{k=0}^{\lfloor d/3 \rfloor} \sum_{m=0}^{d-3k} \binom{\lfloor d/3 \rfloor}{k} \binom{d-3k}{m} Q\left(\sqrt{\frac{d+2k+4m}{5}\frac{E_s}{N_0}}\right) \quad (2)$$

where $I_d = \sum_{k=0}^{\lfloor d/3 \rfloor} \sum_{m=0}^{d-3k} \binom{\lfloor d/3 \rfloor}{k}\binom{d-3k}{m}$. P_d for 64-QAM can be derived following the same procedure, and is not repeated here due to space limitations.

Fig. 2 compares bounds computed using the approach described above and simulation results for convolutional-coded BICM with BPSK, QPSK, 16-QAM and 64-QAM. The simulation implements the BICM scheme defined in the 802.11n standard [1]. As we can observe, the bounds are tight when the decoded BER is less than 10^{-2}.

The bounds for PER (or codeword error probability) can be similarly derived as $P_{cw} \leq \sum_d A_d P_d$, where P_d is computed as described above and A_d is the number of weight-d codewords [19].

Authorized licensed use limited to: CLEMSON UNIVERSITY. Downloaded on July 15,2024 at 19:51:40 UTC from IEEE Xplore. Restrictions apply.

Charter Communications, Inc.
Exhibit 1014
Page #2

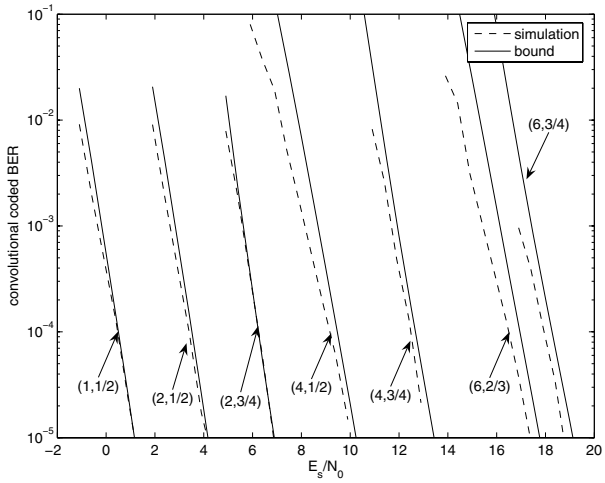

Fig. 2. Comparison of bounds and simulation results for bit-interleaved convolutional-coded modulations over the AWGN channel. (m, R) denotes m bits per symbol and code rate of R.

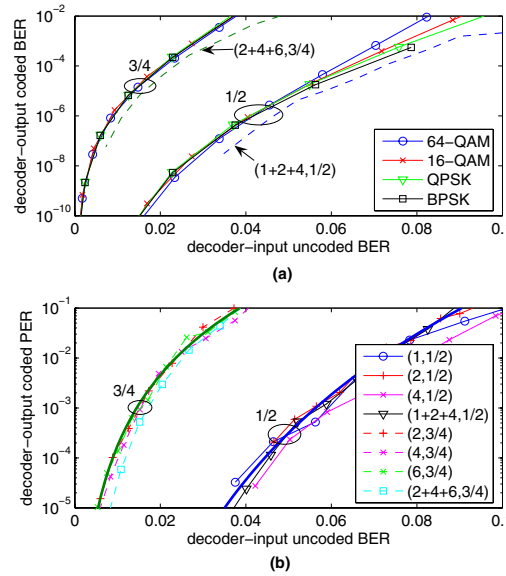

Fig. 3. (a) Performance bounds (solid lines) and simulations (dashed lines) of coded BER vs. uncoded BER for punctured (1/2,7) convolutional code over the AWGN channel with different modulation schemes. (b) Simulations (dashed lines) of coded PER vs. uncoded BER for punctured (1/2,7) convolutional code over the AWGN channel with different modulation schemes. The two bold lines in (b) are log-linear approximations given in Table I.

IV. BER Estimation of Convolutional Coded MIMO Transmission with MMSE Detection

The indoor channel for 802.11 is well known to be a slow fading channel [16], where all OFDM symbols in one packet experience approximately the same channel. As discussed previously, we can apply the well known Gaussian approximation [14] to the MMSE detector output, and normalize it to be an unscaled AWGN channel. channel. As a result, for any IEEE indoor channel, the AWGN model is applicable for each packet, and the bounds derived above can be directly applied to the 802.11n BICM system.

A. The Relationship Between Decoder-Output BER/PER and Decoder-Input BER

In 802.11n, all spatial streams share one (or two) decoder(s), although spatial streams may have different modulation schemes. As a result, each codeword may be modulated by different modulation types. Thus, to be able to analyze the coded performance in this scenario, we need to derive a relationship between the decoder-output BER/PER and input modulation schemes. Our goal is to find a simple algorithm that can compute the decoder-output BER/PER in real time. Reference [17] examines decoder-output BER/PER as a function of decoder-input mutual information. In the present paper we study decoder-output BER/PER as a function of decoder-input BER.

We find that the mapping between decoder-output BER/PER and the decoder-input BER effectively characterizes the performance of the punctured CCs under consideration. This function is essentially independent of the modulation type. As an illustration, we demonstrate performance of systems with two different coding rates, rate 1/2 and 3/4. We apply combinations of BPSK, QPSK, and 16-QAM to the output of a rate-1/2 CC (denoted by (1+2+4,1/2)), and we apply combinations of QPSK, 16-QAM, and 64-QAM to the output of a rate-3/4 CC (denoted by (2+4+6,3/4)). The slight difference in the modulation sets is because the standard [1] does not allow rate 1/2 for 64-QAM, and only allows rate 1/2 for BPSK. However, the results presented in this paper allow these two cases.

Fig. 3(a) plots performance bounds (solid lines) of decoder-output BER vs. decoder-input BER for all modulation schemes and rates 1/2 and 3/4 over the AWGN channel. It is interesting to observe that at low BER (i.e., decoder-output BER $< 10^{-3}$), for the same code rate, the performance bounds for different modulation schemes remains essentially identical. Also included in the figure are the simulated performance (dashed lines) of MCS (1+2+4,1/2) and (2+4+6,3/4) as described above. The performance of a single code with different modulation types also follow bounds closely. It is very clear from this plot that we can approximate the decoder-output BER as a function of decoder-input BER and coding rate independent of the modulation type, without loss of much accuracy.

To facilitate hardware implementation, we employ simple log-linear approximations of the mapping between decoder-output and decoder-input BER's. Specifically, the decoder-output log-BER $L_{out} = \log(P_{bo})$ is related to the decoder-input log-BER $L_{in} = \log(P_{bi})$ by

$$L_{out} = a_1 L_{in} + a_2 \tag{3}$$

where a_1 and a_2 are listed in Table I as a function of the coding rate R.

Authorized licensed use limited to: CLEMSON UNIVERSITY. Downloaded on July 15,2024 at 19:51:40 UTC from IEEE Xplore. Restrictions apply.

Charter Communications, Inc.
Exhibit 1014
Page #3

Table I. Coefficients of log-linear approximation for decoder-output BER/PER $e^{L_{out}}$ as a function of decoder-input BER $e^{L_{in}}$.

	coded BER as output				coded PER as output			
R	1/2	2/3	3/4	5/6	1/2	2/3	3/4	5/6
a_1	9	6.4	5	4	9.7	6.5	4.7	4
a_2	15	12	10	8.5	21	15.4	13	11.7

A similar situation holds for the mapping of PER vs. decoder-input BER, as shown in Fig. 3(b). The two bold lines are log-linear approximations, whose coefficients are also listed in Table I. Alternatively, a simple lookup table can be constructed from Figs. 3(a) and 3(b).

B. Computation of Decoder-Input BER

Since the standard does not allow adaptation in the frequency domain, the MIMO channels carried by each of the OFDM subcarriers have the same set of modulation schemes (each spatial stream may have a different modulation type). We can combine spatial data from different subcarriers of a common spatial stream (with an identical modulation type), and determine its BER using well known formulas [19]. Then the final decoder-input BER of mixed spatial streams can be computed from BER's of different spatial streams.

Specifically, to compute the log-decoder-input BER L_{in}, let b_k be the number of bits per symbol for the k-th spatial stream and P_k^u be the uncoded BER corresponding to the k-th spatial stream. It is easy to show that

$$L_{in} = \log\left(\sum_{k=1}^{N_{ss}} P_k^u b_k\right) - \log\left(\sum_{k=1}^{N_{ss}} b_k\right) \tag{4}$$

The expressions for P_k^u for the modulation schemes defined in 802.11 are well known to be a function of the standard Q-function. To enable fast hardware computations and to retain high accuracy, we again employ log-linear approximation of $Q(\sqrt{x})$, rather than the common exponential upper bound. Since for most applications the decoder-output BER ranges between 10^{-10} and 10^{-3}, which corresponds to the range of decoder-input BER from 10^{-3} to 0.1, we optimize the log-linear approximation of Q-function only in this range. We find that $Q(\sqrt{x}) \approx 0.23e^{-x/1.75}$ approximates well.

To compute P_u^k for the k-th spatial stream combined from different subcarriers, let the uncoded BER for the k-th spatial stream over the m-th subcarrier be $P_{k,m}^u$. We may write

$$P_k^u = \frac{1}{N_d}\sum_{m\in I_d} P_{k,m}^u \tag{5}$$

where I_d is the index set for data subcarriers, and $|I_d| = N_d$. Since N_d is often large, e.g. 52 for 20MHz, and the probabilities $P_{k,m}^u$ involve exponential functions, (5) may be too computationally intensive for real-time situations.

For each subcarrier, $P_{k,m}^u$ is a function of the SNR $\rho_{k,m}$ (post-processing SNR, signal-to-interference-plus-noise ratio to be more specific) for that particular carrier. Ideally speaking, it is desirable that we find an equivalent SNR ρ_k for the spatial stream combined from all subcarriers so that P_k^u can be directly computed using ρ_k, as the same stream at all subcarriers are modulated using the same modulation scheme.

Let $\rho_{min,k} = \min_m\{\rho_{k,m}\}$ and $\rho_{mean,k} = \sum_m \rho_{k,m}/N_d$. Since the channel may be quite frequency-selective, the SNR's for different subcarriers may vary over a very large range. For those carriers with SNR larger than $\rho_{mean,k}$, their contributions in (5) are essentially negligible. The remaining probabilities mostly fall within the range of an order of magnitude, where it is easy to verify that their geometric mean is very close to their arithmetic mean. Utilizing this fact and the exponential approximation of the Q-function discussed earlier, we have

$$\rho_k \approx \frac{2}{N_d}\sum_{m:\rho_{k,m}<\rho_{mean,k}} \rho_{k,m} \tag{6}$$

Simulation confirms that the above expression indeed approximates the true equivalent SNR closely. In fact, an even simpler linear approximation of the above expression

$$\rho_k \approx \frac{1}{2}\left(\rho_{mean,k} + \rho_{min,k}\right) \tag{7}$$

also works very well in simulations for uncoded BER from 10^{-3} to 10^{-1}, as will be demonstrated later.

To compute the uncoded BER at the OFDM demodulator output for a spatial stream of the MIMO channel at one subcarrier, since the MMSE output is known to be well approximated as Gaussian, we employ expressions for the AWGN channel to compute the detector output BER. For the k-th spatial stream at a subcarrier, the normalized MMSE detector output can be written as $Y_k = X_k + \widetilde{W}_k$ where $\widetilde{W}_k$ is the total interference plus noise, and it is approximated as correlated Gaussian. When per-tone channel estimation is employed, its power can be easily derived as

$$E\left[\left|\widetilde{W}_k\right|^2\right] = \frac{\sum_{i\neq k}|G_{k,i}|^2}{|G_{k,k}|^2} + \frac{1+2N_{ss}\sum_l\left(\mathbf{P}^{-T}\right)_{k,l}^2}{|G_{k,k}|^2}N_0\sum_l|H_{k,l}|^2 \tag{8}$$

where omitting the subcarrier index, $\mathbf{H}$ is the channel matrix and $\mathbf{G}$ is the MMSE equalizer matrix. $\mathbf{P}$ is the high-throughput (HT) long-training-field (LTF) preamble permutation matrix defined in [1]. If perfect channel estimation is employed, $\sum_l\left(\mathbf{P}^{-T}\right)_{k,l}^2$ can be replaced by zero. This variance should also be adjusted accordingly in presence of carrier-frequency offset or other impairments.

Fig. 4 compares the scatter plot of the measured and predicted uncoded BER as a function of the proposed simple SNR metric (7) for QPSK over IEEE channel model 'B' [16], with four transmit and two receive antennas. There are two spatial streams, with STBC employed. The two groups of points correspond to the two spatial streams. For the stream with lower BER, the proposed metric is very accurate. For the stream with higher BER, the proposed simple metric provides a slightly conservative estimate, because high SNR's are ignored in (7).

V. The Link Adaptation Algorithm

Upon receiving a packet, the receiver can immediately estimate and predict the channel for the next arriving packet. As discussed earlier, since the indoor channel is a slow fading channel, the channel for consecutive packets undergoes a small amount of change, which can be approximated by a linear

Authorized licensed use limited to: CLEMSON UNIVERSITY. Downloaded on July 15,2024 at 19:51:40 UTC from IEEE Xplore. Restrictions apply.

Charter Communications, Inc.
Exhibit 1014
Page #4

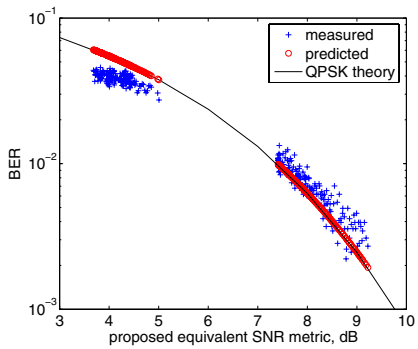

Fig. 4. Scatter plot comparison of BER computed with the proposed simple metric and the exact BER for a 4x2 system.

model, i.e., $\hat{\mathbf{H}}_{next} = \mathbf{H}_{current} + \frac{L_{current}}{L_{prev}} \Delta\mathbf{H}$ where $L_{current}$ and L_{prev} are packet lengths for the current and previous packets, respectively. $\Delta\mathbf{H}$ is the difference between the current and the previous channels. This channel prediction approach can be directly employed for the equivalent frequency-domain channel per subcarrier with and without space-time coding.

The MCS of the current packet can also be estimated from the HT signal field preamble [1]. The same MCS is initially assumed for the next packet, and the PHY performance can be predicted by first estimating the uncoded performance and then the coded performance. If the predicted coded performance cannot satisfy the performance requirement requested by the application, then the algorithm instructs the link adaptation unit to search MCS for a lower throughput. Otherwise, if predicted performance is better than the required performance, then throughput increase should be attempted, which guarantees that the throughput will be maximized. The MCS update algorithm searches the MCS table based on predefined algorithms. The available MCS is constrained by the number of transmit and receive antennas and maximum supportable N_{ss}.

The MCS search algorithm consists of two parts, construction of the MCS table and the MCS search routine. Since the MCS set defined by the standard contains MCS's of duplicate throughput, the MCS table implemented may be simplified by choosing the one with the best performance among all MCS's of the same rate. For example, MCS (4,4,3/4), (6,2,1/2) and (6,2,3/4) may not be necessary to use in practice since the same throughput can be achieved with MCS (4,2,1/2), (4,4,1/2) and (4,4,3/4) respectively, with equivalent or better performance.

When operating at very low SNRs, it may be necessary to reduce the number of spatial streams to sustain performance. As an example, for a maximum of two spatial streams, MCS (1,1,1/2) can be switched to MCS (1,1/2) or (2,1/2) if MCS (1,1,1/2) can not satisfy performance requirement. On the other hand, if MCS (4,3/4) can be satisfied, then MCS (2,2,1/2) or (4,2,1/2) can be selected for upgrading to two spatial streams.

To search MCS in the MCS table, several different approaches can be implemented. The trivial one is exhaustive search. Every entry in the MCS table is tested following the direction of search, and the algorithm stops until a suitable choice is found.

When MCS of identical modulation types across all spatial streams is employed, a simpler search routine is possible. One key observation that can be obtained from Fig. 2 is that, for a higher modulation level, i.e., larger number of bits per symbol, the performance achieved with the lowest coding rate is always better than the lower modulation level coded with highest rate. This phenomenon holds true generally over all IEEE models. As a result, the search for MCS can be substantially simplified: the type of modulation can be selected separately from the rate of code.

The situation is different when unequal MCS (different modulation type for different spatial streams) is employed. We can no longer use modulation-first approach. We instead should consider the modulation-coding product (MCP) which is the product of the total bits per symbol of modulation schemes and the coding rate. MCP indicates the equivalent bits per symbol of the combined MCS. As an example, for $N_{ss} = 2$, entries of the constructed MCS table from low MCP to high MCP are (1,1,1/2), (2,2,1/2), (4,2,1/2), (4,4,1/2), (6,4,1/2), (4,4,3/4), (6,4,3/4), (6,6,2/3), (6,6,3/4) and (6,6,5/6), with MCP being 1, 2, 3, 4, 5, 6, 7.5, 8, and 9 respectively.

A faster search routine can be devised for the above MCS table. As an example, in a throughput increasing trend, for MCS (4,4,1/2), instead of moving to MCS (6,4,1/2), the algorithm can check directly whether a coding rate of 3/4 can be supported with four bits per symbol in both streams. If it can be supported , then there is no need to check MCS (6, 4, 1/2), and the algorithm should directly check MCS (6,4,3/4) for the next step. Otherwise, the algorithm checks MCS (6,4,1/2).

VI. Results and Discussion

We simulated the proposed link adaptation technique over IEEE channel model 'B' [16] for a system with four transmit and two receive antennas and maximum two spatial streams. No retransmission is employed. The system has 20 MHz physical bandwidth and employs space-time coding and unequal MCS. This limits the maximum throughput to be no more than 130 Mbps with a 800 ns guard interval (GI) [1]. Beamforming and antenna selection are not employed, and we implement MMSE detection of the transmitted data. We assume perfect synchronization and timing. The transmission nonlinearities are also ignored. Below, SNR refers to average SNR per receive antenna. The fast search algorithm discussed above is used in simulations.

In the simulations, the data length is 2500 bytes per packet. To have a more realistic simulation, each bursty transmission of consecutive packets is limited to have no more than 1000 packets per burst. The channel for different bursts are uncorrelated. For simulation of each SNR point, around 20000 packets are transmitted over the channel.

For a BER target of 5×10^{-4} which corresponds to a PER target around 3×10^{-2}, Fig. 5 shows the error-rate performance of the system at 10 dB. In this simulation, we assume perfect channel estimation. In a good channel condition, a maximum of 39 Mbps can be achieved. The average throughput for this

Authorized licensed use limited to: CLEMSON UNIVERSITY. Downloaded on July 15,2024 at 19:51:40 UTC from IEEE Xplore. Restrictions apply.

Charter Communications, Inc.
Exhibit 1014
Page #5

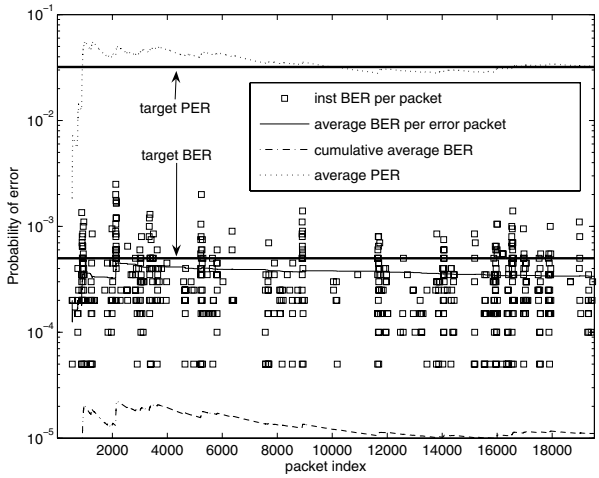

Fig. 5. Error rate performance at SNR = 10 dB.

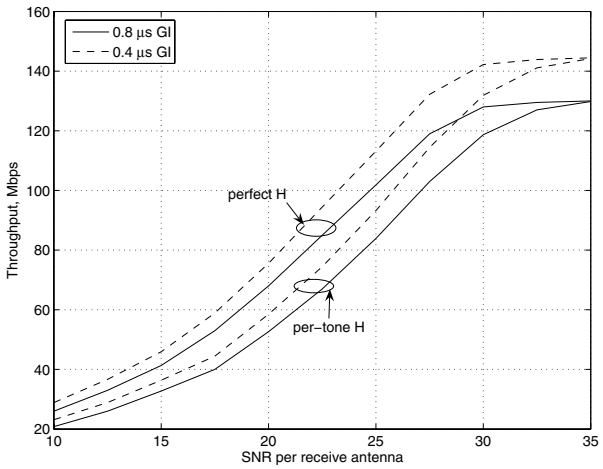

Fig. 6. Throughput of 20MHz-bandwidth 802.11n system of two spatial-streams with the proposed link adaptation technique over IEEE channel model 'B'. Essentially error-free communication is achieved with these throughputs. STBC and unequal MCS is employed. PER target is 10^{-3}.

simulation is around 30 Mbps, which is around twice that for a single fixed MCS at this SNR satisfying the same performance requirement. At the same time, the PER target of 0.03 is achieved as shown in Fig. 5. The average BER for failed packets is also kept just below the BER target of 5×10^{-4}, as intended in the MCS selection process.

Fig. 6 shows the throughput performance of the system with a target PER of 10^{-3} and BER of 10^{-5}. Notice that the BER target is less than $1/(\text{data length})$, which yields essentially error-free communication. In the simulations, there are no more than four packets with errors among 20000 simulated packets. With the more stringent performance requirement, the throughput at 10 dB is about 26 Mbps that is slightly lower than the one in the previous example. With per-tone channel estimation, similar performance is achieved at the expense of lower throughput. The loss of performance due to channel estimation error is less than 3 dB as expected, which can be reduced with better channel estimation techniques, such as least-squares channel estimation.

VII. Conclusion

We have proposed a simple link adaptation technique that maximizes throughput while satisfying the application performance requirement for the receiver PHY/MAC. We employ log-linear approximations for computing the receiver PHY performance, which can be implemented by very simple hardware. We showed that the coded performance can be modeled as a function of the the decoder-input uncoded BER and the coding rate. We have also illustrated how to compute this uncoded BER and proposed a simple SNR metric for computing the BER for spatial streams mixed from different OFDM subcarriers.

References

[1] IEEE 802.11 working group, *IEEEP802.11n/D0.02*, Feb 2006.
[2] G. Caire, G. Taricco and E. Biglieri, "Bit interleaved coded modulation," *IEEE Trans. Info. Theory*, vol 44, no1, pp. 927-946, May 1998.
[3] P. Ormerci, X. Liu, D. L. Goeckel and R. D. Wesel, "Adaptive bit-interleaved coded modulation," *IEEE Trans. Commun.*, vol 49, no 9, pp. 1572-1581, Sep 2001.
[4] S. M. Alamouti and S. Kallel, "Adaptive trellis-coded multiple-phase-shift keying for Rayleigh fading channels," IEEE Trans. Commun., vol 42, no 6, pp. 2305-2314, June 1994.
[5] Y. Li, Y.-C. Liang, S. Sun and R. Zhang, "Adaptive trellis and bit-interleaved coded modulation for ordered MIMO-OFDM channels," *IEEE 16th Int. Symp. PIMRC*, pp. 226-230, 2005.
[6] X. Li, H. Huang, G. J. Foschini and R. A. Valenzuela, "Effects of iterative detection and decoding on the performance of BLAST,", *IEEE GlobeCom 2000*, pp. 1061-1066, Nov 2000.
[7] C. Hermosilla and L. Szczecinski, "Adaptive modulation and coding for turbo receivers in space-time BICM," *IEEE WCNC 2006*, pp. 1293-1298, Las Vegas, NV, April 2006.
[8] S. ten Brink, "Convergence behavior of iteratively decoded parallel concatenated codes," *IEEE Trans. Commun.*, vol 49, pp. 1727-1737, Oct 2001.
[9] K.-B. Song, A. Ekbal, S. T. Chung and J. M. Cioffi, "Adaptive modulation and coding for bit-interleaved coded OFDM," *IEEE Int. Conf. Commun. (ICC)*, June 2004.
[10] P. Xia, S. Zhou, and G. B. Giannakis, "Adaptive MIMO-OFDM based on partial channel state information," *IEEE Trans. Signal Processing*, vol 25, no 1, pp. 202 - 213, Jan 2004.
[11] Y. T. Hwang, C. Y. Tsai and C. C. Lin, "Block-wise adaptive modulation for OFDM WLAN systems," *IEEE ISCAS 2005* pp. 6098-6101, May 2005.
[12] T. C. W. Schenk, G. Dolmans, D. Modonesi, "Throughput of a MIMO-OFDM based WLAN systems," *SCVT2004*, Gent, Belgium, Nov 2004.
[13] G. Taricco and E. Biglieri, "Space-time decoding with imperfect channel estimation," IEEE Trans. Wireless Commun., vol 4, pp. 1874-1888, July 2005.
[14] X. Wang and H. V. Poor, "Iterative (turbo) soft interference cancellation and decoding for coded CDMA," *IEEE Trans. Commun.*, vol 47, pp. 1046-1061, July, 1999.
[15] F. Peng and J. Zhang, "Performance-based link adaptation systems," US patent pending, filed by Renesas Solutions Corp., 2006.
[16] IEEE 802.11 TGn channel model special committee, "TGn Channel Models for IEEE 802.11 WLANs", *IEEE doc.: IEEE 802.11-03/940r4*, May 2004.
[17] Y. Li and W. E. Ryan, "Mutual-information-based adaptive bit-loading algorithms for LDPC coded OFDM,", to appear, *IEEE Trans. Wireless Commun.*, 2006. (Also published in *WNCG'04*, Austin, TX, Oct 2004)
[18] P. W. Wolniansky et al, "V-BLAST: An architecture for realizing very high data rates over the rich-scattering wireless channel", invited paper, *Proceedings of ISSSE Conference*, Pisa, Italy, September 1998
[19] J. G. Proakis, *Digital Communications*, 4th ed, McGraw-Hill, 2000
[20] M. G. Kim, "On systematic punctured convolutional codes," *IEEE Trans. Commun.*, vol 45, no 2, pp.133-139, Feb 1997.

Authorized licensed use limited to: CLEMSON UNIVERSITY. Downloaded on July 15,2024 at 19:51:40 UTC from IEEE Xplore. Restrictions apply.

Charter Communications, Inc.
Exhibit 1014
Page #6